Conference on Nuclear Cross Sections and Technology Washington, 3-7 March 1975.

CEA-Conf--3001

FISSION THEORY AND ACTINIDE FISSION DATA

A. Michaudon
Service de Physique Nucléaire - Centre d'Etudes de Bruyères-le-Châtel
B.P n° 61 - 92120 Montrouge , France

Abstract

The understanding of the fission process has made great progress recently, as a result of the calculation of fission barriers, using the Strutinsky prescription . Double-humped shapes were obtained for nuclei in the actinide region . Such shapes could explain, in a coherent manner, many different phenomena : fission isomers, structure in near-threshold fission cross sections and anisotropy in the emission of the fission fragments . A brief review of fission barrier calculations and relevant experimental data is presented. Calculations of fission cross sections, using double-humped barrier shapes and fission channel properties, as obtained from the data discussed previously, are given for some U and Pu isotopes .

The fission channel theory of A. Bohr has greatly influenced the study of low-energy fission .However, recent investigation of the yields of prompt neutrons and γrays emitted in the resonances of ^{235}U and ^{239}Pu, together with the spin determination for many resonances of these two nuclei cannot be explained purely in terms of the Bohr theory . Variation in the prompt neutron and γ-ray yields from resonance to resonance does not seem to be due to such fission channels, as was thought previously, but to the effect of the (n, γ f) reaction .

The number of prompt fission neutrons and the kinetic energy of the fission fragments are affected by the energy balance and damping or viscosity effects in the last stage of the fission process, from saddle point to scission . These effects are discussed for some nuclei, especially for ^{240}Pu .

1 - Introduction

The design of nuclear reactors, especially for the fast breeders, requires the knowledge of a great variety of accurate fission data ; among them are i) the neutron-induced reactions for the fuel elements and for the transuranic nuclei formed during the operation of the reactor ii) the average number $\bar{\nu}_p$ and the spectrum of the prompt neutrons which are emitted per fission . These data are often needed over a wide range of incident neutron energies (for example from thermal energy to 20 MeV) and sometimes with an accuracy equal to or better than 1 % . It is obvious that such data cannot be obtained from the nuclear theory of a very complex phenomenon which is not very well known yet, despite extensive studies carried out for more than 35 years . Therefore, most of the accurate fission data come from measurements supplemented by evaluation . But fission theory plays an important role . It is essential, indeed, to have a good understanding of the fission process in order to know what the available fission data actually mean and to treat them adequately . For example, the intermediate structure effect in some subthreshold fission cross sections has changed completely the picture previously accepted of statistical properties of fission resonance parameters . This effect had not been understood until double-humped fission barrier shapes were obtained in Strutinsky's calculations and a new fission mechanism was proposed .Also, calculations based on reliable fission models, hence on fission theory, are needed to provide good evaluated fission data not only by fitting the experimental data but also and mainly by interpolating and extrapolating the known data to energy regions and/or to nuclei where no experimental results are available yet . This type of "model calculations" is more and more used by the evaluators and must be based on good fission theory .

An extensive and detailed assessment of the contribution of fission theory to fission data is largely beyond the scope of this paper . Rather, we shall focus our attention on some aspects of the fission process which may be useful for obtaining or understanding various fission data . This explains the following organization of the talk :

- Fission barriers (static and dynamical aspects) .
- Fission channel theory of Bohr .Application to the ^{239}Pu resonances . The (n,γ f) reaction .
- Damping effects . Application to the fission of ^{240}Pu at low energy .

2 - Fission barriers

2.A - The fission barrier of a nucleus is determined from the knowledge of the multidimensional potential energy surface over a wide range of deformations, from the ground state to scission through the saddle point . This potential energy cannot yet be calculated accurately by fundamental methods . Though Hartree-Fock methods are making rapid progress for the treatment of largely deformed nuclear systems[1] , they cannot be used at present to calculate fission barriers with a good precision . The most reliable method consists in using the phenomenological prescription of Strutinsky[2] in which the total energy $E_{(s)}$ of the nuclear system at a given deformation (s) is obtained by adding to the liquid drop energy E_{LD} ((s)) a shell energy correction ΔE_{sh} ((s)) which takes into account the bunching of the single-particle levels near the Fermi surface :

$$E_{(s)} = E_{LD}((s)) + \Delta E_{sh}((s)) \qquad (1)$$

Several groups are actively engaged in such macroscopic-microscopic calculations in which the correction ΔE_{sh} ((s)) is obtained by using different types of shell-model potentials : Harmonic oscillator[2,3] , Woods-Saxon[4] , folded Yukawa[5] , two-centre potentials[6,7,8] . These calculations give fission barrier shapes with two humps for nuclei in the actinide region, as is illustrated in Fig.1 . Such barrier shapes can explain in a coherent manner many different aspectyof the fission phenomenon which were discovered independently one from another, for example : fission isomers, intermediate structure in subthreshold fission cross sections, structure in near-threshold fission cross sections, angular distribution of the fission fragments . This subject has been treated already in several review papers[9,10,11,12] .

2.B - Let us sum up the main aspects of the situation. About 45 fission isomers have been identified in nuclei from U through Cf isotopes with half-lives between 5.10^{-11} s. (^{242}Cm) and $1.4.10^{-2}$ s. (^{241}Am)
The subnanosecond time region has been explored for even-even U and Cm fissiun isomers using a geometrical magnifying effect in the fission-in-flight method[13] . No doubt that other fission isomers having shorter life-times and formed with lower isomeric ratios could be observed using improved techniques . Strong odd-even effects in the life-time values, sometimes as large as 10^3 in ratio, are observed for most of the

fission isomers . It is not clear at present whether these effects are due to a change in barrier height (as modified by pairing and/or specialization energies) or in barrier penetration (i.e. a different curvature and/or mass inertia parameters) or both . Detailed fission description of the fission isomers seems to come not only from the ground state but also from excited states in the second well of the fission barrier . Prompt γ ray transition between excited states of the ground state rotational band in the second well, preceding delayed fission deexcitation, has been detected through conversion electrons for the 4 ns ^{240}Pu fission isomer[14]. The low value of their measured energy gives the first piece of evidence that the fission isomers have a large amount of inertia, hence a large deformation, in agreement with the double humped barrier representation[14]. The γ ray decay of a shape isomer by tunneling through the inner barrier (the β - branch) has been observed for ^{238}U (ref.15). Information on the spin and parity I^{π} of the fission isomers is extremely scarce . Indication on the I^{π} values for some of them is obtained from the angular distributions of the anisotropy of the fission fragments[16,17] . Unambiguous I^{π} values are very difficult to determine since i) several combinations of I and K quantum numbers can fit the data ii) it is not sure that value of K for the nuclear system is conserved when crossing the outer barrier and iii) the initial alignment of the compound nucleus formed by the reaction can be modified by neutrons and γ rays emitted before the formation of the shape isomer and also by the perturbation brought about by extra nuclear fields .

The intermediate structure in subthreshold fission cross sections has been observed for several non-fissile isotopes (a review of the subject is given in[9]) This phenomenon has been interpreted as being due to the existence of compound nucleus states in the second well of the double-humped fission barrier (class-II states)[18] as is illustrated in Fig.2 . The fine structure of the narrow resonances due to the compound nucleus states in the first well (class-I states) is then modulated by the coupling of these states to the fission exit channels through the class-II states acting as intermediate states . According to this proposed mechanism, all the large fission resonances belonging to a given cluster should have the same spin, that of the class-II state responsible for their enhanced fission width . This has been verified experimentally for ^{237}Np where the intermediate structure effect is quite pronounced[19] and where the "s" wave resonances can have two J values (J=2 and 3) . An unambiguous experiment using polarized neutrons and a polarized ^{237}Np target, clearly demonstrates that the fission contribution in the first cluster at 40 eV comes essentially from one spin state (J=3) (See Fig. 3)[20] . This mechanism also predicts that, in a given cluster, the large fission resonances should have their fission widths distributed, on the average, along a lorentzian, as a function of incident neutron energy . In addition to this smooth behavior these fission widths should exhibit Porter-Thomas fluctuations . Such a distribution is actually observed in presently available data[9,21] .

Analysis of available fission data relevant to an interpretation in terms of the double-humped barrier can yield information on barrier parameters such as the heights of the two maxima and of the second minimum relative to the energy of the ground state . Comparison of such "experimental" fission barrier parameters with calculated values shows in general, good overall agreement but with a few areas of discrepancies ; for instance, in the Th region , the measured inner barrier is definitely higher than all values obtained from calculations[9] .

Another interesting aspect to investigate in the potential energy landscape of the fissioning nucleus is the behavior of the surface as a function of odd deformation parameters . It is a well known fact that low energy fission is an asymmetric fragmentation for most actinides except for the lighter ones where a mixture of symmetric and asymmetric yields can appear (see ^{227}Ac, for example) and also for ^{258}Fm which seems to prefer symmetric fragmentation only . Compilation of fragment mass distributions for the actinides shows also that, for increasing mass of the fissioning nucleus, the leading side of the heavy fragment peak forms very stable (around Z=50 and N=82) whereas the light fragment peak moves toward higher masses . These features seem connected to shell effects but an satisfactory explanation could be provided before extensive calculations for odd and even deformation parameters, using the Strutinsky prescription, could be available . An illustration of calculations of this type is shown for ^{240}Pu in Fig.4[8] , where it can be seen that asymmetry in the fission fragment yields is apparent in the potential energy surface at scission . A closer examination of the picture indicates that asymetry in the nuclear system already appears at the second saddle point, between the shape isomer and scission, where a double valley starts to develop and deepens for increasing deformation as the shell structure of the nascent fragments plays a more important role due to a more pronounced necking-in . Comparison of experimental mass distributions with those obtained from such calculations shows qualitative agreement . In particular, it is of interest to note that, for light actinides (^{226}Ac), the threshold for symetric fission appears a few MeV higher than that for asymetric fission[22] . Nevertheless, a quantitative account of the experimental results cannot be obtained from the theory yet[22],especially since these potential energy calculations should be supplemented by a satisfactory theory of the fission dynamics which is started being studied .

2.C - The calculation of fission cross sections or fission lifetimes (for example for the ground state), requires the knowledge of the equation of motion for the fissioning system all the way to scission . This cannot be achieved without some theory of fission dynamics which, on the other hand, is poorly understood at present. One does not even know what type of fission dynamics is to be applied since it seems to depend strongly on the excitation energy (See Section 4). In the absence of an appropriate theory, one is led to make very crude assumptions in actual calculations .

- At low energy, in the sub-barrier region, it is generally assumed that the phase corresponding to the crossing of the barrier (i.e. where E({s}) is greater than the energy E of the system)is adiabatic. This hypothesis means that the fission mode does not induce real intrinsic excitations in the system. After the crossing of the barrier, when the nucleus moves, in an irreversible manner, from the point of exit (where E = E ({s})) to scission, the fastness of the process is such that the adiabatic approximation is questionable. Viscosity effects may then appear in which real intrinsic excitations can be produced due to their coupling to the fission mode . These effects can affect the properties of the fragments (kinetic and excitation energies) but do not modify the fission probability since they appear in the last stage of the process only.

- At higher excitation energy, above the barrier, the situation is more complicated since viscosity (or damping) effects can appear at a much earlier stage of the process and therefore modify the value of the fission probability . In this energy range, general use is made of the Bohr-Wheeler formula :

$$2\pi \frac{\langle \Gamma_f \rangle}{\langle D \rangle} = N_f \qquad (2)$$

- $\langle \Gamma_f \rangle$ and $\langle \Gamma_n \rangle$ are respectively the average fission width and spacing of the compound nucleus states taken into account ,

and - N_f is the number of states available at the saddle point .

This formula, which will be discussed in more detail in section 4, is derived by assuming statistical equilibrium and is generally verified experimentally . It has been pointed out, nevertheless, that this relation requires finite viscosity for the collective motion .

Let us now comment on these two hypotheses and illustrate how they can be used for the calculation of some fission data .

- The adiabatic approach is certainly justified for the calculation of life times $T_{g.s}$ for spontaneous fission of nuclei in their ground state . In that case, the fission probability λ per unit time ($\lambda = (T_{g.s})^{-1}$) is equal to the frequency $\frac{1}{2\pi}\omega_f$ for the zero point motion mode, multiplied by the barrier penetrability P .

$$\lambda = \frac{1}{2\pi}\omega_f \times P \qquad (3)$$

In actual calculations, it is generally assumed that $\frac{1}{2\pi}\omega_f = 0.5$ MeV and the value of P can be obtained by standard WKB techniques[25] . The calculations of P are greatly simplified for one dimensional fission barriers and constant mass parameters B . One then obtains :

$$P \simeq \exp\left(-2\frac{S}{\hbar}\right) \text{ if } S \gg \hbar \qquad (4)$$

with $$S = \int_{s'}^{s''} \sqrt{2\,|E - E(s)|}\cdot B \cdot ds \qquad (5)$$

In this last expression :

- s is the deformation parameter along the fission path .
- s' and s" (with s" > s') are the values of s, respectively at the entrance and exit of the barrier for which the total energy E of the system is equal to that of the barrier ($E = E(s') = E(s")$) .

Improvements to life-time calculations have been brought about recently by a more sophisticated approach [4,26], that we shall summarize below .

It is first considered that the potential energy is known in a multidimensional space with a set $\{s\} = (s_1, s_2, \ldots s_i \ldots s_j \ldots)$ of deformation coordinates, using the Strutinsky procedure . But the major step forward is to consider that the mass inertia parameter B is no longer constant but can vary with $\{s\}$. This is justified by noting that the shell structure, which is so important in the calculation of the potential energy also plays a major role in the value of the mass tensor B_{ij} (the indices i and j refer to the deformation coordinates s_i and s_j respectively) . Actual calculations of B_{ij}, using the "cranking" formula show oscillations in these values with deformation quite similar to those of ΔE_{Sh} discussed previously . In this multidimensional representation, with possible variations in B_{ij} with $\{s\}$ taken into account explicitly, the expression for S now reads :

$$S = \int_{\sigma'}^{\sigma''} \sqrt{2\,|E - E(\{s\})|}\; B(\sigma)\, d\sigma \qquad (6)$$

where :

- the deformation parameters s_i, s_j, are supposed to be functions of some arbitrary parameter σ .
- σ' and σ'' are the end-point values of the parameter σ , similar to s' and s" defined in (5), for which $E = E(\sigma') = E(\sigma'')$.
- $B(\sigma)$ is the effective mass defined by the following relation :

$$B(s) = \sum_{i,j} B_{ij}\left(s_1(s), s_2(s) \ldots s_i(s) \ldots s_j(s) \ldots\right) \frac{ds_i}{d\sigma}\frac{ds_j}{d\sigma} \qquad (7)$$

In the "static" approximation, the collective motion in the fission mode is supposed to be slow enough so that, for each deformation $\{s\}$, (for a given E value) the nucleons have enough time to rearrange themselves . It is then justified to consider the state of the system (including the single particle states $|\omega\rangle$) at any deformation $\{s\}$ in the sub barrier region . In these conditions, it is possible to derive an expression for B_{ij} , in terms of the single particle states $|\omega\rangle$, having eigenvalue ϵ_ω, using the following formula :

$$B_{ij}(s) = 2\hbar^2 \sum_{\omega,\omega'} \frac{\langle\omega|\frac{\partial}{\partial s_i}|\omega'\rangle\langle\omega'|\frac{\partial}{\partial s_j}|\omega\rangle}{\epsilon_{\omega'} - \epsilon_\omega} \qquad (8)$$

The calculation of s_i with equation (6), can be carried out provided that a trajectory, the fission path, is defined between the two end points σ' and σ'' . If B had a constant value, the fission path would follow the external values of the potential energy surface . This condition defines what is called the "static barrier" . The fission path is no longer the static barrier if B varies with deformation . For example, the fission trajectory may reach higher potential energy if the mass parameter takes there a smaller value . The fission path is then determined by the least-action principle ,which leads to the smallest possible value for S and, consequently, for $T_{g.s}$. Such a path gives the so-called "dynamical barrier" which is illustrated in Fig.5 for ^{240}Pu. It is interesting to note that the least-action trajectory does not pass through the "static" saddle points, but prefers a path at a somewhat higher energy . This seems to apply to most of the cases studied so far and appears to be a consequence of a large mass parameter at the saddle point . This effect itself is due to the shell structure which gives a large positive shell-energy correction at that deformation .

The validity of this method can be checked by comparing the fission life-time values obtained from such calculations with the experimental ones . This comparison must be carried out with great care since, according to the authors themselves[4,26] the calculations seem to be extremely sensitive to both microscopic and macroscopic properties of the nucleus . Some of these properties are not well known and the uncertainty associated with their values can drastically change the results of the calculations .For example,the variation of the pairing strength with deformation is practically unknown but plays a crucial role in the derivation of the mass tensor B_{ij} from expression (8) . In the absence of more detailed information, it is generally assumed that the pairing strength is either constant or proportional to the surface area of the nucleus. But switching from one to the other of these two assumptions changes the $T_{g.s}$ values by an enormous factor, from 8 to 10 orders of magnitude for Uranium isotopes . A change as small as 10 % in the pairing strength can bring about as large as about five orders of magnitude in the life-time determination . Such variations can be expected in the deformation dependence of the pairing strength . For example, self-consistent calculations of the properties of Sm isotopes for various deformations, using the Hartree-Fock-Bogolyubov method with external constraint, show oscillations in the pairing strength as high as 20 % over a limited range of deformations, much smaller than that met in fission[28]. Also, the liquid drop parameters need to be correctly adjusted to reproduce the experimental data. For example, in Fig.6, where a good overall agreement is achieved between experimental and calculated values of $T_{g.s}$, not only a simple assumption was made on pairing but also the reduced fissility parameter ζ,as defined in[5], had to be adjusted separately for the various series of isotopes

Therefore, it would seem that this very interesting method needs to be complemented by a more accurate knowledge of both microscopic (pairing strength) and macroscopic (fission barriers) properties of the fissioning nucleus as a function of deformation .

The difficulty in calculating, from basic theory, such a simple quantity as the fission half-life for the ground state is still very pronounced for the calculation of fission cross sections. For example, the theory cannot predict as yet the detailed sequence and the exact energies of the available transition states above the two saddle points of the double humped barrier. All practical calculations make very crude assumptions about the physical quantities which are needed. In fact, most of the calculations still assume a single humped barrier with a constant level parameter a .

A more sophisticated approach, though far from being completely satisfactory, has been developed recently in terms of the double humped shape, including damping in the two wells of the barrier, and in which the physical quantities needed in the calculations are adjusted by fitting as many relevant fission data as possible[29]. We summarize below this method which makes use of the statistical model for the calculation of the neutron cross sections (including that for fission) of heavy nuclei between 1 keV and 1 MeV .

The main difficulty of the calculations lies in the determination of the fission probability at a given energy and for a well-defined set $\{c\}$ of quantum numbers (generally J,π,M and r). For all sets $\{c\}$, one-dimensional fission barriers are considered, all of them having the same shape, as sketched in Fig.7 . This shape is obtained by smoothly joining three parabolas having parameters extracted from fits to relevant fission data such as those discussed in Section 2[9,30]. For each set $\{c\}$, the barrier is shifted as a whole of an energy $\Delta E(\{c\})$ determined by the fitting procedure. Damping is introduced through the form of an imaginary part in the potential in order to simulate the coupling of the fission mode to the intrinsic degrees of freedom .

The transmission of the barrier is calculated by solving the Schrödinger equation in the complex potential thus obtained .

The experimental data Di, used in this procedure when they are available, are the following :

- D_1 - the total fission cross section $\sigma_f(E_n)$ at incident neutron energy E_n .
- D_2 - the angular distribution $\sigma_f(\theta, E_n)$ of the fission fragments emitted at angle θ relative to the direction of the incident neutron beam .
- D_3 - the coefficients $a_L(E_n)$ of the Legendre polynomial expansion $\sigma_f(\theta, E_n) = \sum_L a_L(E_n) \cdot P_L(\cos\theta)$ used to fit the $\sigma_f(\theta, E_n)$ data .
- D_4 - The anisotropy $a_s(E_n) = \sigma_f(0°, E_n) / \sigma_f(90°, E_n)$

The fission parameters Pi , determined by fitting the above data are :

- P_1 - the energy shift $\Delta E(\{c\})$ for the lowest fission channel having quantum numbers $\{c\}$.
- P_2 - the effective number $N(\{c\})$ of fission channels having quantum numbers $\{c\}$. This takes into account the possible opening of more fission channels for increasing E_n .
- P_3 - the coefficients α_n of an analytical expression $N(\{c\}) = f(E_n, \alpha_n)$ describing the variation of $N(\{c\})$ with E_n .
- P_4 - the maximum depth W_m of the imaginary part of the potential supposed to have a parabolic shape, in the 2nd well.(Full damping is assumed in the first well)

These parameters Pi are determined by a least-square fit to the data Dj . In order to simplify the fitting procedure, only the most important of the 16 combinations Pi x Dj are taken into account, those which connect the available data Dj with the most sensitive parameters Pi .

Illustration of the results obtained in such calculations is given in Fig. 8 and 9 where the calculated fission and capture cross sections for ^{239}U, ^{238}Pu and ^{240}Pu are plotted as a function of E_n . Other cross sections such as those for elastic and inelastic scattering are also obtained with this procedure . All the cross sections are calculated by using a coupled channel optical model potential with the parameters obtained by fitting ^{238}U data (ref. 31) .

It is interesting to note that not only the calculated results are in agreement with the experimental data (in fact most of the data have been used in the fitting procedure) but also that this method can give calculated cross sections where no experimental data are available (for example $\sigma(n, f)$ for ^{232}U, ^{236}U and ^{238}Pu).

In summary, despite the lack of a good fission theory to calculate fission data such as life times or cross sections, it is nevertheless possible to make use of the fairly good knowledge of the fission barriers and of simple fission models provided that their parameters can be adjusted to accurate and relevant experimental data . We shall now discuss the fission theory of A.Bohr which is commonly used in the interpretation and the calculation of fission data .

3 - Fission Channel Theory of A. Bohr : Application to ^{239}Pu resonances - The $(n, \gamma f)$ reaction .

As we have seen in Section 2, it is far beyond the present capabilities of fission theory to predict the fission properties of a specific fissioning state having spin and parity J^π and at an excitation energy above the neutron emission threshold and, a fortiori, to predict how these properties vary with J^π . Nevertheless, a simplification in this very complex problem appeared when A. Bohr showed that many properties of the fission process through these individual excited states could be discussed in terms of a small set of reaction alternatives or channels, even though the number of different fragment pairs is very large in binary fission of a heavy nucleus[32]. In this approach, A. Bohr proposed the concept of fission exit channels by considering that the passage from saddle point to scission is so rapid that the properties of fission, though strongly dependent on several factors, are nevertheless influenced by those of the transition states at the saddle point. In this picture, the fission exit channels are therefore these transition states whose spectrum, according to A. Bohr, is very similar to that of the first excited states of the nucleus at ground-state deformation .

This channel theory of fission provides also another interpretation of the number N_f of fission exit channels[23]. This concept of "open" fission channels was expressed in terms of fission saddle-point configurations which were energetically available . Their number N_f is given by expression (7) . This expression simply comes from the fact that the ensemble of nucleons finds itself in all allowed configurations (including the N saddle-point configurations) once every period $\tau \sim 2\pi\hbar / \langle D \rangle$. The life time τ_f for fission is thus $\tau_f \sim 2\pi\hbar / N\langle D \rangle$ from which the average fission width and Eq.(2) are then deduced .

Within the framework of the channel theory of Bohr, an effective number of fission channels, called $(N_{eff})_J^\pi$, is now defined for each spin and parity J^π . This number $(N_{eff})_J^\pi$ is also expressed in terms of the average fission width and spacing as in (2) , but, in addition, is equal to the sum of the penetrabilities Pi

for each fission channel i having spin and parity J^π. Each P_j is calculated for the fission barrier associated with the transition state j. Thus :

$$(\Gamma_{ff})_{J^\pi} = \gamma \frac{\langle \Gamma_f \rangle_{J^\pi}}{\langle D \rangle_{J^\pi}} = \gamma \sum_i P_i \qquad (9)$$

Let us now examine how the predictions of the Bohr theory are verified in the case of ^{239}Pu resonances which are fairly well known (including their spin J) and for which the fission channel properties are very different for the two possible J^π values ($J^\pi = 0^+$ and 1^+) obtained in the capture of "s"-wave neutrons by ^{239}Pu, whereas the lowest $J^\pi = 0^+$ transition state is symmetric and below the neutron separation energy S_n in ^{240}Pu (this is in fact the ground state of the system), the lowest $J^\pi = 1^+$ transition state seems to be asymmetric, since it has been postulated to be a combination of the two $K^\pi = 0^-$ and $K^\pi = 1^-$ octupole vibrations, and at an excitation energy above S_n.

The discussion of this subject, as already published in a previous paper[9], is summarized below and supplemented by new results obtained for prompt neutron and γ-ray emission in the ^{239}Pu resonances.

The fission width distribution for the ^{239}Pu resonances shows, as for the other fissile nuclei, large fluctuations due to the small number of available fission exit channels defined in terms of the Bohr theory. But, in contrast to all similar distributions, the one for ^{239}Pu shows clearly a break, explained by the existence of two families of resonances having widely different average fission width values. This interpretation is supported by the spin determination for a large number of resonances, as obtained by both direct and indirect methods. The values of γ_{eff}, for $J^\pi = 0^+$ and 1^+ from the average widths and spacings of the resonances are respectively $(\gamma_{eff})_{0^+} = 1.43$ and $(\gamma_{eff})_{1^+} = 0.07$. This is in agreement with the Bohr theory if the existence of a 1^+ transition state of collective character is postulated below the 2-quasi-particle excitations.

The different symmetry properties of the transition states should be reflected in the fission properties of the 0^+ and 1^+ resonances.

The mass distribution of the fission products was measured by the "wheel technique" using a nuclear explosion as a pulsed-neutron source[33]. By radiochemical analysis, the valley-to-peak ratio of the mass distribution, or more exactly the $^{115}Cd/^{99}Mo$ ratio R was obtained for more than twenty resonances with energies ranging from 15 to 82 eV. The R-values seem to fall into two categories having average values of R in ratio 3.5. High and low values of R are associated respectively with 0^+ and 1^+ spin states, in agreement with the theory. Moreover, there is also a correlation between the R values and the fission widths, as expected : the fission widths are larger, on the average for the group of resonances having high values of R (Fig. 10).

Variations of the total kinetic energy of the fission fragments were observed and they can also be correlated with the spin states and the variations of R in the way predicted by theory of Bohr[34].

The behavior of $\bar{\nu}$, the average number of prompt neutrons per fission, from resonance to resonance, has been more difficult to understand for quite a long time. The situation was very puzzling several years ago when the most complete set of data available at that time showed definite variations in $\bar{\nu}$, but in opposite directions[35,36]. Moreover, these variations could be correlated with J, but in a different manner ; the high values of $\bar{\nu}$ were associated with $J^\pi = 1^+$ for one set of data[35] but with $J^\pi = 0^+$ for the other one[36]. Nevertheless, both results could find an interpretation in terms of the Bohr theory. For one case[35] it is possible to justify the observed correlation between $\bar{\nu}$ and J^π by postulating that, neglecting viscosity effects, the fission barrier associated with the 1^+ transition state remains higher than for $J^\pi = 0^+$ all the way to scission. This energy difference can thus be found in an increase in the excitation energy of the fission fragments, hence in a larger $\bar{\nu}$ value. A different argument can be invoked to explain the other set of results[36] ; since the 1^+ transition state is asymmetric, a more asymmetric mass division is expected and is actually found for the 1^+ resonances, as we discussed above. This effect should be accompanied by a lower value due to the well known sawtooth behavior of $\bar{\nu}(A_f)$ as a function of the fragment mass A_f (ref.37).

This confusion was not dissipated by other experiments, carried out a little later, since they concluded to the existence of fluctuations, but not correlated with J^π[38,39]. The situation has been clarified by more recent measurements of $\bar{\nu}$ and E_γ, the mean γ-ray energy emitted per fission[40,41]. The Saclay results[40] were obtained by using a big (570 l) Gd-loaded liquid scintillator for the detection of the prompt neutrons and γ rays emitted per fission. Large fluctuations are observed both in $\bar{\nu}$ and $\bar{E}_\gamma$ measured values which appear to be strongly anticorrelated. This means that high values are generally associated with low $\bar{\Gamma}_\gamma$ values. These data can be better understood if they are plotted separately for the 0^+ and 1^+ resonances which have been analysed below 200 eV. The fluctuations in $\bar{\nu}$ and $\bar{E}_\gamma$ values together with the anticorrelation between these two quantities clearly appear for the 1^+ resonances (see Fig.11) but are much less significant for the 0^+ resonances. Statistical tests applied to these data confirm this effect. The probability that the fluctuations in $\bar{\nu}$ and $\bar{E}_\gamma$ are of purely statistical nature is below 5.10^{-5} for the 1^+ resonances but as large as 0.1 and 0.63 respectively for the $\bar{\nu}$ and $\bar{E}_\gamma$ values of the 0^+ resonances. Also the correlation coefficient between $\bar{\nu}_i$ and $\bar{E}_{\gamma i}$, for a set of resonances i, is -0.84 and 0.07 respectively for the two sets of 1^+ and 0^+ resonances. There is respectively 7 % and 77 % probability that these two coefficients can be caused by statistical fluctuations only.

A closer examination of the data shows that the fluctuations in $\bar{\nu}$ and $\bar{E}_\gamma$ are larger for the 1^+ resonances having smaller fission widths. This effect appears more clearly in Fig.12 where both $\bar{\nu}$ and $\bar{E}_\gamma$ are consistent with a linear dependence with $1/\Gamma_f$.

An interpretation of this phenomenon has been put forward[42] in terms of the $(n,\gamma f)$ reaction already considered in a more general context[43]. The width $\Gamma_{\gamma f}$ for the reaction $(n,\gamma f)$ is expected to be fairly small (a few meV according to calculations[43]) and constant from resonance to resonance since it corresponds to a many-exit-channel process. It may occur that, due to the large fluctuations of Γ_f discussed previously, $\Gamma_{\gamma f}$ becomes comparable to Γ_f for some resonances, more likely to have $J^\pi = 1^+$ rather than $J^\pi = 0^+$ since $\langle \Gamma_f \rangle_{0^+} \gg \langle \Gamma_f \rangle_{1^+}$. For these resonances, the $(n,\gamma f)$ process competes with comparable probability with "direct fission", called (n,fd) in which the initial compound nucleus deexcites directly by fission. This competition explains the properties observed in $\bar{\nu}$ and $\bar{E}_\gamma$. In the $(n,\gamma f)$ reaction, more γ rays and therefore less neutrons are emitted because i) γ rays are emitted before scission by the compound nucleus which is thus less excited and ii) the final γ-ray emission by the fragments below their neutron emission threshold is common to both $(n,\gamma f)$ and $(n,f\,d)$ processes.

These considerations lead to the following relations :

$$\Gamma_f = \Gamma_{\gamma f} + \Gamma_{fd} \qquad (10)$$

$$\overline{\Gamma_{\gamma f}} = \overline{E}_{\gamma fd} + \overline{e}_{\gamma} \qquad (11)$$

$$\overline{\nu}_{fi} = \overline{\nu}_{fd} - \overline{e}_{\gamma} \frac{\partial \overline{\nu}_i}{\partial E^*} \qquad (12)$$

where - the subscripts f, γf and fd refer to the total fission, (n,γf) and (n,f d) processes

- $\frac{\partial \overline{\nu}_i}{\partial E^*}$ is the variation of $\overline{\nu}_i$ with excitation energy E^* in "direct fission"

- $\overline{e}_{\gamma}$ is the mean energy of the pre-scission γrays emitted in the (n, γf) reaction

In the resonances where the (n,γf) and (n,f d) reactions compete, the neutron and γ ray yields are as follows :

$$\overline{E}_{\gamma} = \overline{E}_{\gamma fd} + \overline{e}_{\gamma} \, \Gamma_{\gamma f}/\Gamma_f \qquad (13)$$

$$\overline{\nu} = \overline{\nu}_{fd} - \overline{e}_{\gamma} \frac{\partial \overline{\nu}}{\partial E^*} \cdot \Gamma_{\gamma f}/\Gamma_f \qquad (14)$$

These calculated yields show a linear variation with $\Gamma_{\gamma f}/\Gamma_f$ which is actually found in the experimental results for the 1^+ resonances. The phenomenon is certainly present in the $J^\pi = 0^+$ resonances but is masked by their large fission width .

This seems to be *the first piece of evidence* for the existence of the (n, γf) reaction which is also confirmed by the fact that the average multiplicity $\overline{n}_{\gamma}$ of the fission γ rays emitted in the ^{239}Pu resonances shows a linear dependence with $\Gamma_{\gamma f}/\Gamma_f$ in the same manner as $\overline{\nu}$ and $\overline{E}_{\gamma}$ [42] .

Analysis of the $\overline{\nu}$ and $\overline{E}_{\gamma}$ data, by a least-square fit to the experimental values, is consistent with the conservation of the energy for the sum of the prompt neutron and γ-ray yields. This analysis gives the following value :

$$\Gamma_{\gamma f} \cdot \overline{e}_{\gamma} = (4.6 \pm 0.4) \times 10^3 \text{ eV}^2 \quad (J^\pi = 1^+) \qquad (15)$$

For the 0^+ resonances, a similar expression can be derived though the phenomenon is much less pronounced :

$$\Gamma_{\gamma f} \cdot \overline{e}_{\gamma} = (8.0 \pm 1.9) \times 10^3 \text{ eV}^2 \quad (J^\pi = 0^+) \qquad (16)$$

These values are in agreement with recent calculations making conventional assumptions about the fission and γ-ray decay of compound nucleus states[40] .

The existence and the influence of the (n, γf) reaction for the ^{239}Pu resonances seems to be clearly established and explains most of the variations observed in $\overline{\nu}$ and $\overline{E}_{\gamma}$. It explains also the fact that no resonances have been observed with a fission width smaller than 4 meV, which is very close to the expected value for $\Gamma_{\gamma f}$.

After removal of the effect of the (n, γf) reaction in the ^{239}Pu resonances, one obtains for the neutron and γ-ray yields and for the two spin states :

$$(\overline{\nu}_{fd})_{0^+} - (\overline{\nu}_{fd})_{1^+} = 0.0130 \pm 0.0055 \text{ neutrons} \qquad (17)$$

$$(\overline{E}_{\gamma fd})_{0^+} - (\overline{E}_{\gamma fd})_{1^+} = 10 \pm 10 \text{ keV} \qquad (18)$$

This results in the following difference in the excitation energy E_f^x for the fission fragments and for the two spin states :

$$(E_f^x)_{0^+} - (E_f^x)_{1^+} = 109 \pm 43 \text{ keV} \qquad (19)$$

It seems therefore that there is a weak effect of the fission exit channels on the prompt neutron and possibly on the γ-ray yields and also on the excitation energy of the fission fragments .

Similar studies have been carried out on ^{235}U (ref. 40) and ^{241}Pu (ref. 44) but show much smaller effects in the first case and practically none in the second case.

In summary, the fission channel theory of A. Bohr seems generally verified in the fission data, in particular for the case of the ^{239}Pu resonances which are fairly well known . A careful study of the prompt fission neutron yields supplemented by that of the prompt fission γ rays, in the ^{239}Pu resonances, has clarified a situation which was previously rather confusing . The fluctuations in $\overline{\nu}$ from resonance to resonance seem to be caused by the (n, γf) reaction rather than by the effect of fission channels .

4 - Damping effects in fission. (Application to the fission of ^{240}Pu at low energy)

A complete theory of fission must take into account not only the static aspects, essentially the potential energy surface as a function of deformation coordinates but also the dynamical aspects which include inertial and damping effects . In Section 2, we described the present status of the potential energy surface which is now known with a relatively good accuracy, in contrast to the dynamics of the process . A discussion of a derivation of mass inertia parameter for spontaneous fission, supposed to be adiabatic during the crossing of the barrier, has shown the limitations of the calculational method. But even less is known about damping or viscosity effects which describe the coupling of the fission mode to other degrees of freedom . It seems that damping is quite large in the first well, moderate in the second well, but very little is known about the damping in the last phase, i.e in the descent from the second saddle point to scission. This information is nevertheless very important for predicting the energy share between the kinetic and excitation energies of the fission fragments and therefore the prompt neutron emission . Many contradictory assumptions have been made between the two following extremes : i) full damping in which all *the available energy at scission is dissipated into* excitation energy with no pre-scission kinetic energy ii) weak damping in which this available energy appears almost completely in the form of pre-scission kinetic energy with at intrinsic excitation of the fissioning system[45,46,47] . It is very difficult to find out from *the experimental results, what type of damping actually* occurs in the descent to scission and how this damping varies with excitation energy . The fragment total kinetic energy $\overline{TKE}$ for the low energy fission of actinides shows a linear dependence with $Z^2\ A^{-1/3}$ over a wide range of mass numbers[49] . Under simple assumptions, the Coulomb energy V_c of the two fragments at scission can also show a linear dependence with $Z^2\ A^{-1/3}$:

$$V_c = \frac{Z_{f1} \times Z_{f2}}{d} e^2 \qquad (20)$$

where :

- Z_{f1} and Z_{f2} are the atomic numbers of the two fragments

and - d is the distance of the two charge centers at scission .

The $Z^2\ A^{-1/3}$ dependence, for a given fragment mass ratio, can be derived by assuming that the distance d is proportional to $A^{1/3}$. One then obtains :

$$V_c \propto \frac{Z^2}{A^{1/3}} \qquad (21)$$

This linear dependence of V_c with $Z^2\ A^{-1/3}$ could suggest that, at scission, there is no appreciable kinetic energy and that the total kinetic energy $\overline{TKE}$ comes from Coulomb repulsion only . This would tend to favor the strong damping hypothesis. Nevertheless, this simple picture is unrealistic as has been pointed out already[47]. In fact, at scission, the distance d depends not only on A but also on Z . For higher Z values,

the scission configuration is relatively more elongated, therefore with lower Coulomb energy . Liquid drop calculations[45] show that the variation of V_c with Z^2/A actually flattens and even decreases for increasing Z^2/A for large Z^2/A values . But, assuming this time the zero damping hypothesis to apply, the pre-scission kinetic energy added to V_c gives $\overline{TKE}$ values which are also in fairly good agreement with the experimental results[45] .

Ternary fission data cannot help much in clarifying this complex situation since they can be explained equally well in terms of either weak damping[50] or full damping[46] .

In spite of our poor knowledge of damping effects in the last phase of fission, let us examine how they can play a role by comparing $\overline{TKE}$ and $\overline{\nu}$ data for spontaneous and neutron-induced fission of some even-even nuclei . Special attention is given to the ^{240}Pu case for which (d,p f) data are also considered[48] .

It can be seen in Fig.13 that, for a given even-even nucleus, $\overline{TKE}$ is systematically higher for thermal-neutron-induced fission than for spontaneous fission . Therefore, the full damping condition is not met for the cases plotted in Fig.13 since the excess S_n of excitation energy for neutron induced fission is found, at least partially, in the form of kinetic energy . But the difference $\Delta\overline{TKE}$ in $\overline{TKE}$ is less than 6 MeV (the approximate value of S_n for such nuclei), implying that some damping can nevertheless occur which causes the rest ($S_n - \Delta\overline{TKE}$) of the excitation energy to appear in the form of dissipation . This is actually reflected in prompt-neutron emission since the $\overline{\nu}$-values, as plotted in Fig.14, are systematically higher for thermal-neutron-induced fission than for spontaneous fission, in agreement with $\overline{TKE}$ data . From these results, it would seem that moderate damping could apply to the low-energy fission of even-even actinides .

A closer examination of neutron-induced-fission for a wide range of neutron energies E_n (below the threshold for second-chance fission) can help to know better what fraction of the increase in excitation energy E^* of the fissioning nucleus goes into fragment excitation and how this fraction varies with E^* . Many studies have been made on the variation of $\overline{\nu}$ with E_n for a great variety of actinides[51] . An illustration of this $\overline{\nu}$ energy dependence for ^{240}Pu is given in Fig.15 where it can be seen that $\overline{\nu}$ increases linearly with E_n . No attention is paid here to the details of the energy dependence, in particular to the fine structure which may exist at low energy, but rather the gross behavior of $\overline{\nu}$ versus E_n is considered . These results show that the excitation energy of the fission fragments increases at a fast rate as a function of the excitation energy E^* . If this effect, probably due to damping , is supposed to be present in the same manner for all excitation energies below S_n, the linear variation of $\overline{\nu}$ with E_n can be extended down to zero-excitation energy to obtain the extrapolated value of $\overline{\nu}$ (called $\overline{\nu}_{ext}$) for spontaneous fission. Comparison of extrapolated and measured values of $\overline{\nu}$ for ^{240}Pu spontaneous fission shows that the first one is lower than the second one (Fig.15). This effect is found for all even-even actinides for which relevant $\overline{\nu}$ data are available (Fig.14) . Therefore, it seems that the amount of damping would decrease for excitation energies somewhat below S_n .

It is possible to pursue further this type of investigation for the low-energy fission of ^{240}Pu since a fairly large amount of experimental results are available on the properties of the fission fragments and their variation with excitation energy[48,52]. The variation of the total kinetic energy $\overline{TKE}$ for the fragments emitted in the low-energy fission of ^{240}Pu is plotted in Fig.15 which includes data for the spontaneous fission of the ground state (G.S), the 4 ns isomeric state (I.S), in the ^{239}Pu thermal neutron induced fission and for the ^{239}Pu (d,p f) reaction. Also, the variation $d\overline{E_K}/d\theta^*$ of the kinetic energy $\overline{E_K}$ of the fission fragments as a function of excitation energy E^* is plotted in Fig.16 for several groups of fragment mass ratios. Moreover the average mass $\langle m_H^* \rangle$ of the heavy primary fission fragments is plotted as a function of E^* in Fig. 17 .

Examination of these data seems to demonstrate the existence of two types of fission . The first one (called type I) includes the G.S and I.S spontaneous fission and ^{239}Pu (d,p f) reaction at $E^* = 4.65$ MeV and for the fragments emitted at an angle $\theta = 0°$ relative to the recoil axis of the ^{240}Pu compound nucleus . A 700 keV wide resonance appears at $E^* = 4.65$ MeV in the anisotropy data and is interpreted as being due to a vibrational level in the 2nd well of the ^{240}Pu double-humped fission barrier. The second one (called type II) refers to all other ^{239}Pu (d, p f) results and to the ^{239}Pu (n,f) reaction induced by thermal neutrons .

In the fission of type I, the kinetic energy $\overline{TKE}$ increases linearly as a function of E^* with a slope of about +1 . This means that practically all the excitation energy E^* is found as an increase of the kinetic energy of the fission fragments and this holds for all types of fragmentations (Fig.16) . The average mass $\langle m_H^* \rangle$ is the same for the three fission reactions of this type . This strongly suggests that damping, if present, must be very small and the fission of type I may very well be an illustration of superfluid motion already envisaged[47] in which the nucleons remain coupled by the pairing force all the way to scission. In this hypothesis, no intrinsic excitation occurs in the descent to scission and the available energy at that point then appears as pre-scission kinetic energy . All increase in E^* is then found entirely as an increase in pre-scission kinetic energy and therefore in $\overline{TKE}$ since the Coulomb energy does not change with E^* in this picture. This applies to all types of fragmentation since all fission properties but the kinetic energy do not vary E^* . The experimental results obtained for fission of the type I are consistent with this superfluid notion of the fissioning system .

In the fission of type II, on the contrary, the kinetic energy $\overline{TKE}$ decreases linearly as a function of E^* with a slope of about -0.43 . This is consistent with the increase of $\overline{\nu}$ with E^* observed above S_n .Nevertheless the energy balance in fission calculated with these data leads to a fairly large value $\langle S_n^f \rangle$ of the average neutron separation energy in the fission fragments ($S_n^f \simeq 8.3$ MeV) . The type of fragmentation is different from that of type I since $\langle m_H^* \rangle$ takes a different value (Fig.17) . There does not seem to be a satisfactory interpretation of such a behavior of $\overline{TKE}$ with and E^* . Several explanations have been proposed in terms either of damping or variation in stiffness of the fission fragments with E^*.[48] In the first case, the coupling of the fission mode to the other degrees of freedom reduces the pre-scission kinetic energy and induces intrinsic excitations which lead to a greater excitation of the fission fragments, hence to an increase in $\overline{\nu}$.[47] In the second case, the greater excitation energy reduces the stiffness of the nascent fragments which then become softer to deform. At scission they are more elongated and the increase in the distance d between their charge centers decreases the Coulomb energy[52,53]. In these interpretations, shell effects seem to play an important role in agreement with the experimental results since the rate of decrease $d\overline{E_K}/dE^*$ of the kinetic energy $\overline{E_K}$ with increasing E^* strongly depends on the fragment mass ratio (Fig.16) .

The existence of these two types of fission having different variations of TFF and $\bar{\nu}$ with excitation energy seems justified from these experimental data and has to be taken into account for the prediction of some fission properties such as the prompt neutron emission. From the discussion presented above, it does not seem correct to assume the same amount of damping in fission for all excitation energies, starting from the ground state. In particular, it is certainly erroneous to extrapolate at higher energy the $\bar{\nu}$ or TFF data obtained for spontaneous and thermal neutron-induced fission.

5 - Conclusion

In summary, though our understanding of the fission process has recently greatly improved, a reliable fission theory does not yet exist ; we are far from completely understanding this very complex phenomenon and from calculating accurately all its properties .

Fission barriers can be calculated with a good accuracy by using the Strutinsky macroscopic-microscopic approach . More fundamental Hartree Fock approaches are also making rapid progress. The double-humped barrier shapes which are obtained for the actinides can explain many aspects of fission, among them are fission isomers and intermediate structure in fission cross sections .

In contrast to the statics, the fission dynamics which includes inertial and damping effects is very poorly known . Attempts to calculate lifetime for ground state spontaneous fission with a microscopic approach have shown the limitations of the method . Fission cross sections are still more difficult to obtain on a fundamental basis . Nevertheless, approximate values can be obtained, not from pure theory, but from simple models having parameters adjusted to selected available fission data . The fission channel theory of A. Bohr, generally verified experimentally, is widely used in such calculations. A similar situation seems to apply also for other fission properties such as prompt neutron emission. Correct treatment of the subject requires the knowledge of damping effects in the descent from the second saddle point to scission. At present one cannot but speculate on such effects though new data on fission fragment kinetic energy and prompt neutron emission start to throw some light on this difficult aspect of fission . Again, in this case, simple models can be used to predict $\bar{\nu}$-values when they are not measured, provided that the model parameters employed in the calculations are adjusted on reliable fission data . But, it has been shown that these data must be used with great care before being introduced in the calculations .

It is worth noting at this point, that damping effects are studied not only in fission but also in heavy-ion induced reactions and a lot of information on such matters is expected in the few years to come when the new heavy-ion accelerators, now under construction, will be put into operation .

References

1 H. Flocard, P. Quentin, D. Vautherin, A.K. Kerman P.C.F.* (IAEA, Vienna 1974) Vol I, p. 231 .

2 V.M. Strutinsky, Nucl. Phys. A 95 (1967), 420 . Nucl. Phys. A 122 (1968), 1 .

3 S.G. Nilsson, Chin Fu Tsang, A. Sobiczewski, Z. Szymanski, S. Wycech, C. Gustafson, I.L. Lamm, P. Möller and B. Nilsson, Nucl. Phys. A 131, (1969),1

4 H. Flocard, J. Bergaard, A.S. Jensen, N.C. Pauli, V.M. Strutinsky and C.Y. Wong, Rev. Mod. Phys. 44, (1972), 320 .

5 J.R. Nix, Ann. Rev. of Nucl. Sc. 22, (1972), 65 .

6 R.I. Andersson, F. Dickmann and K. Dietrich, Nucl. Phys A 159, (1970), 137 .

7 P. Holzer, U. Mosel and W. Greiner, Nucl. Phys.A 138 (1969), 241 .

8 M.C. Mustafa, U. Mosel and H.W. Schmitt, Phys. Rev. C 7 (1973), 1519 .

9 A. Michaudon, Advances in Nuclear Physics - Ed. by M. Baranger and E. Vogt ; Vol 6, p.1 (Plenum Press, 1973) .

10 a) V.M. Strutinsky and N.C. Pauli,P.C.F.** (IAEA,Vienna 1969) p. 155 .
b) J.E. Lynn, P.C.F.** (IAEA, Vienna 1969) p.249 .

11 J.R. Nix, Ann. Rev. of Nucl. Sc. 22, (1972), 65 .

12 a) H.J. Specht, Rev. Mod. Phys. 46 ,No 4 (1974) 773 .
b) V. Metag, E. Liukkonen, D. Glowacz and A. Bergmeister P.C.F.* (IAEA, Vienna 1974) Vol I, p. 317 .

13 P. Linkilde and G. Sletten, Nucl. Phys. A 199 (1973), 306 .

14 H.J. Specht, J. Weber, E. Konecny and D. Heunemann, Phys. Let. B 41, (1972), 43 .

15 P.A. Russo, J. Pedersen and R. Vandenbosch, P.C.F.* (IAEA, Vienna 1974) Vol I, p. 271 .

16 R. Vandenbosch, P.C.F.* (IAEA, Vienna 1974) Vol I, p. 251 .

17 H.J. Specht, E. Konecny, J. Weber and C. Yozhubarov, P.C.F.* (IAEA, Vienna 1974) Vol I, p. 285 .

18 a) J.E. Lynn, Nuclear Structure (IAEA, Vienna 1969) p. 249 .
b) J.E. Lynn, Report A.E.R.E Harwell R 5891 (1968) .
c) H. Weigmann, Z. Phys. 214 (1968), 7 .

19 a) D. Paya, H. Derrien, A. Fubini, A. Michaudon and P. Ribon, Nuclear Data for Reactors (IAEA, Vienna 1967) Vol III, p. 128 .
b) A. Michaudon, Nuclear Structure (IAEA, Vienna 1968) p. 427 .
c) A. Fubini, J. Blons, A. Michaudon and D. Paya, Phys. Rev. Let. 20 (24) (1968) 1373 (C) .

20 G.A. Keyworth, J.R. Lemley, C.E. Olsen, F.T. Seibel, J.W.T. Dabbs, P.C.F.* (IAEA, Vienna 1974) Vol I, p.85.

21 a) A. Michaudon, New Developments in reactor physics and Shielding Calculations, Kiamesha Lake 12-15 Sept 1972, Vol II, p. 1087 - CONF 720-901 .
b) A. Michaudon, Statistical Properties of Nuclei (Albany 23-27 August 1971) (Plenum Press) 1972, p.149

22 E. Konecny, H.J. Specht and J. Weber, P.C.F.* (IAEA, Vienna 1974) Vol II, p. 3 .

* Physics and Chemistry of Fission (Proceedings of a IAEA Symposium; Rochester (N.Y) 13-17 August 1973) .

** Physics and Chemistry of Fission (Proceedings of the second IAEA Symposium, Vienna 28 July-1 August 1969)

[23] N. Bohr and J.A. Wheeler, Phys. Rev. 56 (1939) 426 .
[24] H.A. Kramers, Physica 7 , (1940), 284 .
[25] P.O. Fröman and N. Fröman, J.W.K.B. Approximation, Contribution to the Theory, North Holland, Amsterdam (1965) .
[26] H.C. Pauli and T. Ledergerber, P.C.F.[1] (IAEA, Vienna 1974) Vol I, p. 463 .
[27] D. Inglis, Phys. Rev. 96 , (1954), 1059 .
[28] D. Gogny, private communication (1974) .
[29] a) P. Thuret, JAERI Topical Discussion (Tokyo, March 27, 1974) CEA-conf 2855 .
b) P. Thuret, CEA Report R 4631 (1974) .
[30] H. Weigmann and J.P. Theobald, Nucl. Phys. A 187 , (1972) , 305 .
[31] C. Lagrange, JAERI Topical Discussion (Tokyo, March 27, 1974) CEA conf 2852 - 2853
[32] A. Bohr, Proc. Int. Conf. Peaceful Uses of Atomic Energy (Geneva 1955) Vol II, United Nations, New York (1956) p. 220 .
[33] G.A. Cowan, R.P. Heydorn, R.J. Prestwood, J.S Gilmore and G.M. Rudolph, Phys. Rev. 144 (4), (1966), 979 .
[34] E. Melkonian and G.K. Mehta, P.C.F.[1] (IAEA, Vienna 1965) Vol II, p. 355 .
[35] F.L. Shapiro, Nuclear Structure (IAEA, Vienna 1968) p. 283 .
[36] S. Weinstein, R. Reed and P.C. Block, P.C.F.[1] (IAEA, Vienna 1969) p. 477 .
[37] J. Terrell, Phys. Rev. 127 , (1962), 880 .
[38] L. Weston and J. Todd, Conf. Neutron Cross Sections and Technology (U. of Tennessee, 1971) Vol II, p.961.
[39] J. Trochon, R. Lucas, A. Michaudon, D. Paya and Y. Ryabov, J. Physique 34 , (1973), 131 .
[40] a) D. Shackleton, J. Trochon, J. Fréhaut and H. Le Rigo, Phys. Let. 42 B , (1972), p.344 .
b) J. Fréhaut and D. Shackleton, P.C.F.[1] (IAEA, Vienna 1974) Vol II, p. 201 .
c) D. Shackleton, D. Sc. Thesis (Paris 1974) .
[41] L.W. Weston and J. Todd, Phys. Rev. 10 (4),(1974), 1607 .
[42] a) J. Trochon, Private Communication (1972) .
b) Y. Ryabov, J. Trochon, D. Shackleton and J. Fréhaut Nucl. Phys. A 216 , (1973), 99 .
[43] J.F. Lynn, The Theory of Neutron Resonance Reactions (Clarendon, Oxford, 1968) .
[44] J. Fréhaut, G. Sisan, J. Trochon, Private Communication (1974) .
[45] J.R. Nix, Nucl. Phys. A 130 (1969), 241 .
[46] P. Fong P.C.F.[1] (IAEA, Vienna 1969) p. 133 .
[47] W.J. Swiatecki and S. Bjørnholm, Physics Reports 4, (6) (1972), 325 .
[48] a) J. Lachkar, Y. Patin and J. Sigaud, J. de Physique Lettre (to be published)
b) Journées d'Etudes de la Fission (Cadarache, France 1974) (unpublished) .
[49] R. Vandenbosch and J.R. Huizenga "Nuclear Fission" Academic Press (1973) .
[50] J. Halpern and T.R. Bentley, Comments on Nuclear and Particle Physics 3 , (1969), 57 .
[51] P. Navrro and V.A. Bondin "Atomic Energy Review" (IAEA, Vienna 1972) Vol 10, (4), p.637 .
[52] E. Konecny, H.J. Specht and J. Weber Phys. Let. 45 B, (1973), 329 .
[53] W. Nörenberg, P.C.F.[1] (IAEA, Vienna 1969) p. 51 .
[54] R. Vandenbosch, Comments on Nuclear and Particle Physics , Vol V, (6), (1972), p. 161 .
[55] J.P. Unik, J.E. Gindler, L.E. Glendenin, K.F. Flynn, A. Gorski and R.K. Sjoblom, P.C.F.[1] (IAEA, Vienna 1974) Vol II, p. 19 .
[56] A.J. Deruytter and G. Wegener-Penning P.C.F.[1] (IAEA, Vienna 1974) Vol II, p. 51 .

[***] Physics and Chemistry of Fission (Proceedings of a IAEA Symposium, Salzburg 22-26 March 1965) .

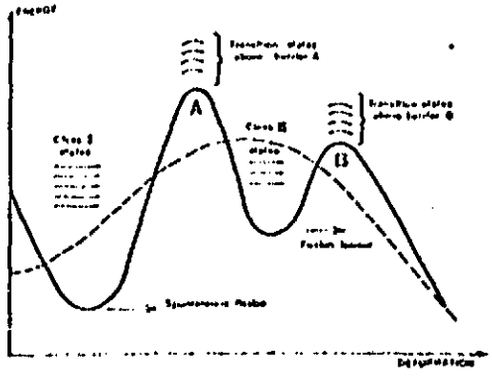

Fig. 1
Double-humped fission barrier (solid line) resulting from shell-energy corrections to the LD barrier (dashed line)

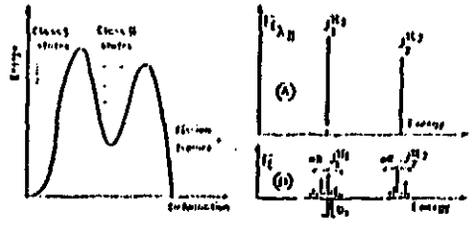

Fig. 2
Mechanism of intermediate structure in subthreshold fission cross sections . Clusters appear in the fission cross section when energy, spin and parity of a class-II state match those of the class-I resonances (at most two J^{π} values are possible for "s" wave neutrons) . The fission widths are drawn at the energy of the respective levels for class-II states (diagram A) and for the observed resonances (diagram B) .

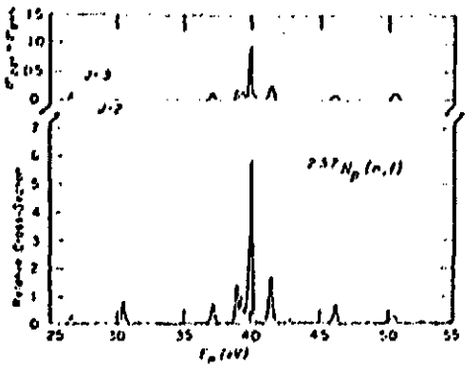

Fig. 3
Fission data obtained in the neighborhood of the first cluster at 40 eV in the ^{237}Np subthreshold fission cross section using a polarized neutron beam and a polarized ^{237}Np target[20]. The upper curve represents the difference between the cross sections measured with beam and target polarizations parallel and antiparallel. These data demonstrate that most of the cross section in this cluster is due to J = 1 resonances[20].

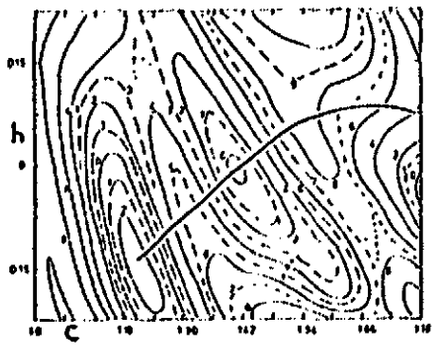

Fig. 5
The calculated deformation energy of ^{240}Pu versus the two symmetric deformations c(elongation) and h (constriction) is shown as a contour plot. Contour intervals are 1 MeV. The projection of the least action trajectory into the symmetric subspace (c,h) is shown by the thick solid line. Note the discrepancy between the static and dynamical barriers[24].

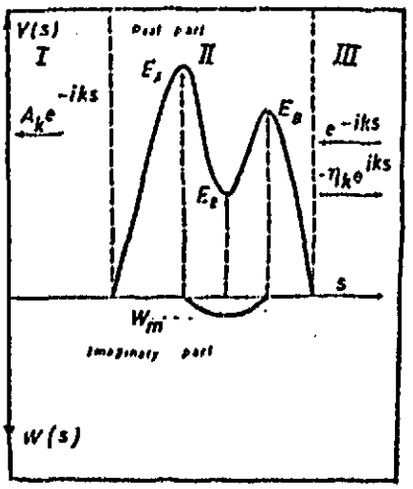

Fig. 7

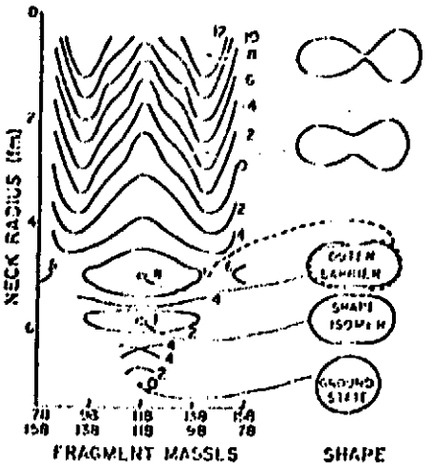

Fig. 4
Potential energy surface for ^{236}U as obtained from calculations using the Strutinsky procedure. Contour intervals are 2 MeV except for the shape isomer 6,54.

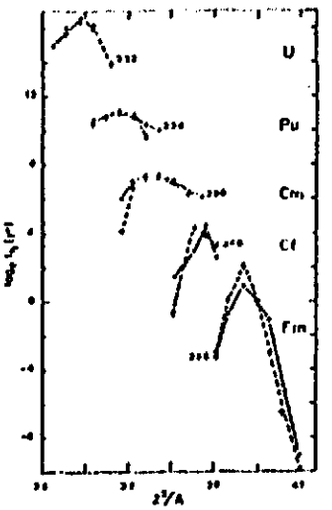

Fig. 6
Theoretical (o) and experimental (+) half-lives (in years) for ground-state spontaneous fission plotted versus Z^2/A (ref.[26]). The parameterization of the fissionability parameter for each set of isotopes is given in [26]. A pairing strength proportional to the surface area of the deformed nucleus is assumed in the calculations.

Fig. 7
Real and imaginary parts of the potential, as a function of deformation s, used in the cross section calculations described in the text and in [29]. The real part V(s) represents the double-humped fission barrier obtained by smoothly joining three paraboles. The imaginary part is supposed to be parabolic with maximum W_m in the second well. Full absorption is assumed in the first well.

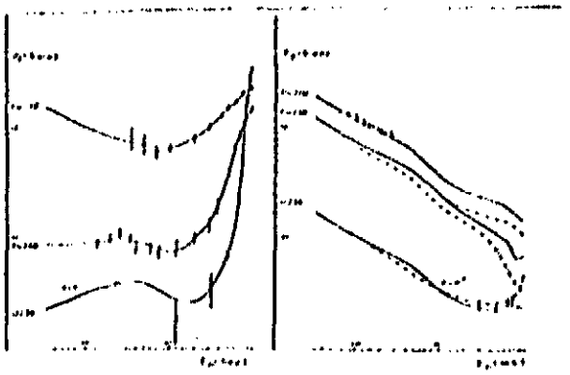

Fig. 8

Fig. 9

Fig. 8 - Fission cross sections of ^{236}U, ^{238}Pu and ^{240}Pu as a function of neutron energy E_n calculated with the method described in [29] (solid lines). The references for the experimental data are given in [29].

Fig. 9 - Capture cross sections of ^{236}U, ^{238}Pu and ^{240}Pu as a function of neutron energy E_n calculated with the method described in [29] (solid lines). The references for the experimental data are given in [29]. The lines - - - come from ENDF/III.

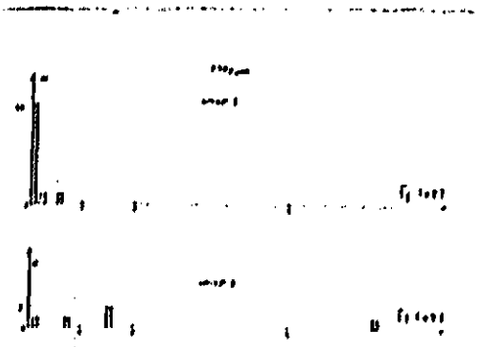

Fig. 10

Frequency distribution of the Γ_f values for the two groups of ^{239}Pu resonances separated according to their R-values, as discussed in the text [9,31].

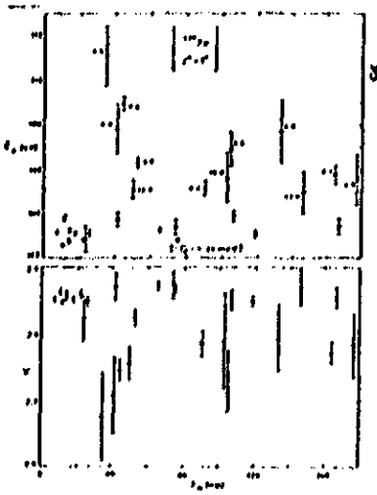

Fig. 11

The fission prompt neutron and γ-ray yields (respectively $\bar{\nu}$ and $\bar{E}_\gamma$) are plotted as a function of resonance energy for the ^{239}Pu resonances having $J^\pi = 1^+$ and analysed below 180 eV neutron energy [40]. The value of Γ_f is indicated in meV near the $\bar{E}_\gamma$ point for the resonances having a small fission width.

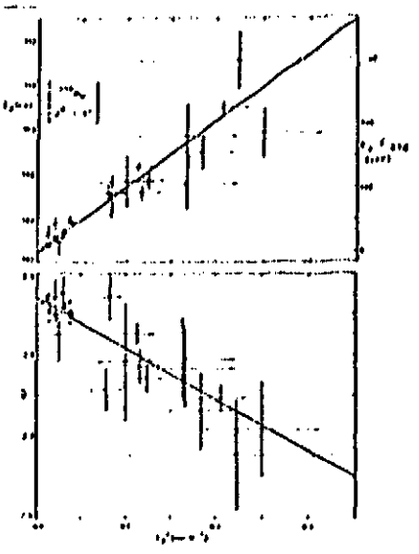

Fig. 12

The prompt-neutron and γ-ray yields (respectively $\bar{\nu}$ and $\bar{E}_\gamma$) are plotted as a function of $1/\Gamma_f$ for the ^{239}Pu resonances having $J^\pi = 1^+$ and analysed below 200 eV neutron energy, to demonstrate the effect of the $(n,\gamma f)$ reaction (ref.40). The solid lines are least-squares fits to the data.

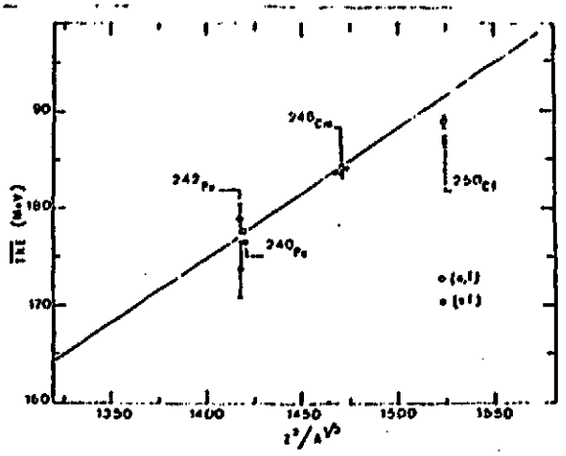

Fig. 13

Comparison of the total kinetic energy $\overline{TKE}$ of the fragments for the ground state spontaneous fission (□) the thermal-neutron-induced fission (○) of some even-even nuclei. The references for these data can be found in [55,56]. The solid line is a fit to the available data [55].

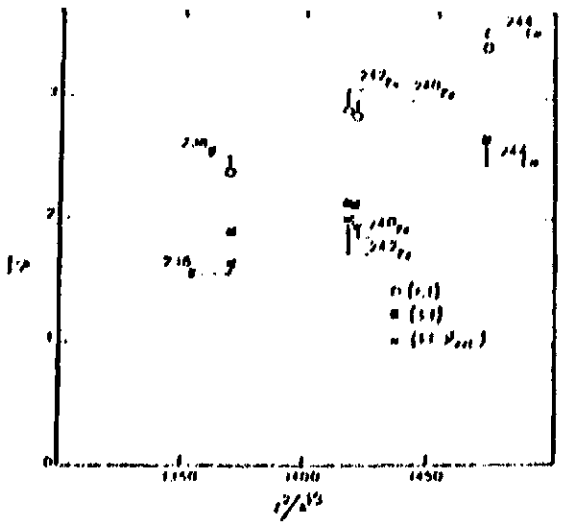

Fig. 14

Comparison of the average fission neutron multiplicity $\bar{\nu}$ for the ground state spontaneous fission (o) and the thermal-neutron induced fission (o) of some even even nuclei. The value $\bar{\nu}_{exc}$ is obtained by extrapolating to zero excitation energy the $\bar{\nu}$ energy dependence observed for the neutron-induced fission .

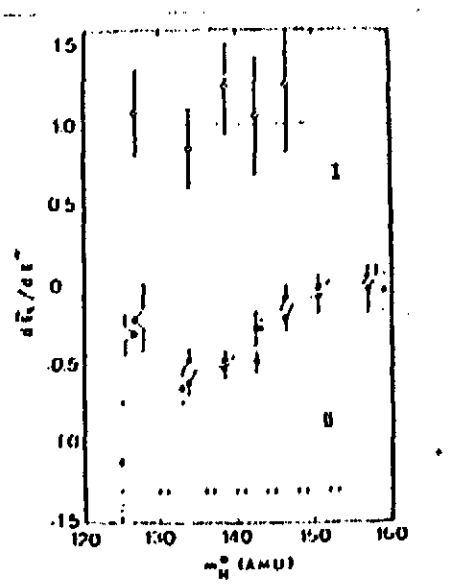

Fig. 16

Variation $\frac{d\overline{E_K}}{dE^*}$ of the fragment kinetic energy $\overline{E_K}$ with excitation energy E^* of the fissioning nucleus ^{240}Pu for various groups of the mass $^*m_H$ of the heavy fission fragment (ref.48) . This variation $\frac{d\overline{E_K}}{dE^*}$ has been plotted for the two types of fission (I and II) discussed in the text. References for the data plotted in this figure can be found in[48] .

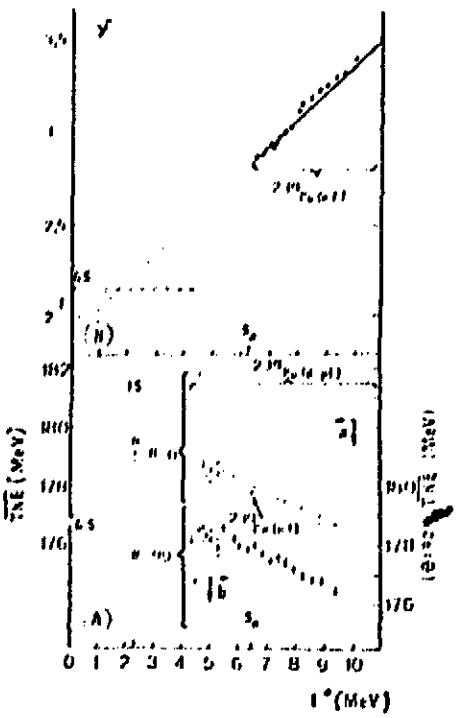

Fig. 15

Plots of the fragment total kinetic energy $\overline{TKE}$ (graph A) and prompt neutron yield $\bar{\nu}$ (graph B) for the fission of ^{240}Pu as a function of excitation energy E^* (ref.48) . *References for the various data plotted in this figure* can be found in[48] .

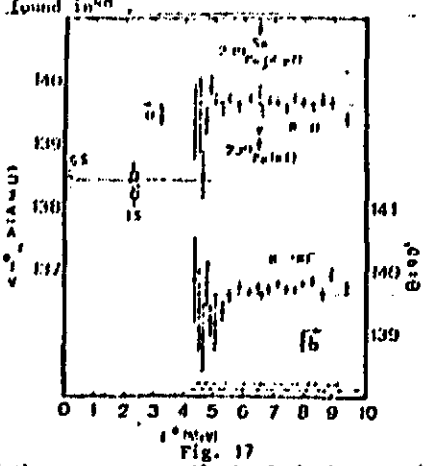

Fig. 17

Plot of the average mass $\langle^* m_H\rangle$ of the heavy primary fragments emitted in the fission of ^{240}Pu as a function of excitation energy E^* (ref. 48). Note the difference in $\langle^* m_H\rangle$ for the two types of fission discussed in the text .